

## Biosorption of Pesticide Onto a Low Cost Carbon Produced from Apricot Stone (*Prunus armeniaca*): Equilibrium, Kinetic and Thermodynamic Studies

Somaia G. Mohammad

*Pesticide Residues and Environmental Pollution Department, Agriculture Research Center, Dokki, Giza, Egypt*

Received: 12 November 2013; Revised: 14 December, 2013; Accepted: 20 December 2013.

© 2013 AENSI PUBLISHER All rights reserved

### ABSTRACT

The biosorption of apricot stone activated carbon (ASAC) from aqueous solution was investigated using low-cost, natural and eco-friendly biosorbent. The biosorption studies were carried out under various parameters, such as biosorbent dosage, initial pesticide concentration, contact time and temperature. The experimental results show that the percentage of biosorption increases with an increase in the biosorbent dosage. The equilibrium uptake was increased with an increase in the initial pesticide concentration in solution. Biosorption kinetic data were fitted well with the pseudo-second order kinetic model. The adsorption isotherms closely followed the Langmuir model. The monolayer adsorption capacity of the apricot stone for ethoprophos was found as 20.04 mg g<sup>-1</sup>. The thermodynamic data indicated that the adsorption of ethoprophos on apricot stone activated carbon was feasible, spontaneous and endothermic in nature. The results revealed that the ASAC could be used as a low cost alternative biosorbent for the pesticide removal from aqueous solution.

*Key words:* Ethoprophos, Apricot stone, Activated carbon, Adsorption isotherm, Kinetics, Thermodynamics.

### INTRODUCTION

In the 21<sup>st</sup> century, environmental pollution is one of the major threats to human life. Pesticides are harmful to life because of their toxicity, carcinogenicity and mutagenicity [19]. The harmful influence of pesticides on human health and the environment has resulted to the imposition of stringent legislation on drinking water quality in many countries Derylo-Marczewska *et al.*, [11].

Ethoprophos (O-ethyl S,S- dipropyl phosphorodithioate) is organophosphorus nematicide and insecticide usually applied for the control of plant parasitic nematodes and soil insects in potatoes, sweet potatoes, tomatoes, vegetables, maize, soybeans, peanuts, bananas, citrus and other crops. The half-life (t<sup>1/2</sup>) of ethoprophos varies from 3 to 30 days. The contamination of surface and ground water by pesticides has become a serious environmental problem in recent years. The toxicity of pesticides and their degradation products is making these chemical substances a potential hazard by contaminating our environment Philip *et al.*, [27]. Therefore, the removal of pesticides from water is one of the major environmental concerns these days.

There are several procedures available for pesticides removal from water which includes photocatalytic degradation Ugurlu and Karaog [33], Gong *et al.*, [16], ultrasound combined with photo-Fenton treatment Katsumata *et al.*, [20], advanced

oxidation processes Zhou *et al.*, [38], aerobic degradation Rajashekara and Manonmani [28], electro dialysis membranes Banasiak *et al.*, [7], ozonation Maldonado *et al.*, [25]. However, these methods are either inefficient or expensive and cannot be used on a large scale. Conversely, biosorption defined as the removal of materials (organic compounds, metal ions, dye molecules, etc.) by inactive, non-living biomass (materials of biological origin) has emerged as an alternative low cost and eco-friendly technology Farooq *et al.*, [14]. This technology is not only economic and simple but also has several advantages such as low initial cost, simplicity of design, ease of operation, insensitivity to toxic substances and complete removal of pollutants even from dilute solutions. In recent years, a number of inexpensive and abundant biosorbents especially agro-waste materials such as pistachio shell Dolas *et al.*, [13], rambutan peel Ahmad and Alrozi [1], mangosteen peel Ahmad and Alrozi [2], corncob Sun and Webley [32], olive-waste cakes Baccar *et al.*, [5], walnut shells Yang and Qiu [35] and different natural products. The advantage of using these waste materials is that it saves disposal costs while alleviating potential environmental problems.

The apricot (*Prunus armeniaca*) is a common fruit in Egypt. The stone fruit cultivated area in Egypt is 49204 ha with an approximate yearly production of 476849 tones (6 % of total fruit

production) Anonymous [3]. Apricot stone as a by-product of the apricot Juice industry is therefore an inexpensive materials. The use of apricot stone as a precursor for activated carbon will provide solution to environmental problems caused by this waste as well as produce a value added product from a low cost material. Therefore, The main object of this study was to examine the feasibility of using the apricot stone activated carbon (ASAC) as a biosorbent for the removal of ethoprophos from the aqueous solution. Effects of different parameters including biosorbent dosage, pesticide concentration, temperature and contact time were studied to

optimize the biosorption process. The isotherm, kinetic and thermodynamic parameters were explored to describe the experimental data.

## Materials and Methods

### 2.1. Adsorbate:

The pesticide used as adsorbate in the experiments is ethoprophos. Some properties and chemical structure of the pesticide is given in Table 1.

**Table 1:** Some properties and chemical structure of ethoprophos.

|                                   |   |
|-----------------------------------|---|
| Common name                       | Ethoprophos   |
| Chemical structure                |   |
| Name                              | O-ethyl S,S-dipropyl phosphorodithioate                       |
| Pesticide group                   | Organophosphorus  |
| Activity                          | Non-systemic nematicide and insecticide                       |
| Molecular formula                 | C <sub>8</sub> H <sub>19</sub> O <sub>2</sub> PS <sub>2</sub> |
| Molecular weight                  | 242.3   |
| Solubility in water at 25°C (g/L) | 700 mg/L  |
| Formulation                       | 10 % GR   |
| Rate of application               | 30 Kg/ Feddan   |

Data were obtained from Tomlin (2004).

### 2.2. Adsorbent (ASAC):

Apricot stone was collected from a local market in Egypt.

### 2.3. Preparation of activated carbon:

Apricot stone used in this study as precursor was sourced locally. These were washed severally with distilled water to remove water-soluble impurities and dried to constant weight in an oven at 70°C for 2 days. The dried samples were ground and sieved by AS 200 Analytical Sieve Shakers, Retsch GmbH, Germany to particle size of 63 µm and further dried in the oven. The sample was then soaked in orthophosphoric acid (H<sub>3</sub>PO<sub>4</sub>) with an impregnation ratio of 1:1 (w/w) for 24 h and dehydrated in an oven overnight at 105°C. The resultant sample was activated in a closed muffle furnace to increase the surface area at 500°C for 2 h. The AC produced was cooled to room temperature and washed with 0.1 M HCl and successively with distilled water. Washing with distilled water was done repeatedly until the pH of the filtrate reached 6–7. The final product was dried in an oven at 105°C for 24 h and stored in a vacuum desiccator until needed Njoku and Hameed [26].

### 2.4. Adsorption experiments:

The adsorption experiments of ethoprophos onto ASAC were carried out in a set of 150 Erlenmeyer flasks. 100 ml of the pesticide solutions of various initial concentrations in the range 30–70 mg/L were

added to separate flasks and a fixed dose of 0.5g of ASAC was added to each flask covered with glass stopper at normal pH 5.48, room temperature (25°C ± 2), for contact time 24h, with occasional agitation to reach equilibrium. The ASAC dose used is the optimum in the range of initial concentrations of pesticide studied and was obtained from preliminary studies.

For kinetic studies of ethoprophos onto ASAC, 100 ml of the solution containing 30–70 mg/L with 0.5g of ASAC for different time intervals from 5 to 300 minutes to determine the equilibrium time. From the triplicate flasks, 40 ml of filtrate was transferred to a separatory funnel and extracted successively three times with 20, 15 and 10 ml portions of dichloromethane. The combined extract was dried on anhydrous sodium sulfate to remove moisture content and evaporated using a rotary evaporator on a water bath at 40°C. The extracted samples were analyzed using GC-FPD.

Isothermal studies of ethoprophos were conducted with an adsorbent quantity of 0.5g of ASAC with pesticide concentrations of 30–70 mg/L in identical conical flasks containing 100 ml of distilled water. Blank solutions were treated similarly (without adsorbent).

### 2.5. Determination of adsorption capacity:

The adsorption capacity was determined by using the following equation, taking into account the concentration difference of the solution at the beginning and at equilibrium Arslanoglu *et al.*, [4].

$$q_e = \frac{(C_0 - C_e)V}{m} \quad (1)$$

Where  $C_0$  and  $C_e$  are the initial and the equilibrium ethoprophos concentration mg/L, respectively,  $V$  is the volume of solution (ml) and  $m$  is the amount of adsorbent used (g).

The percent removal of ethoprophos from solution was calculated by the following equation:

$$\text{Removal percentage} = \frac{C_0 - C_e}{C_0} \times 100 \quad (2)$$

### 2.6. Determination of Ethoprophos concentration:

The concentration of ethoprophos was determined by HP 7890A series Gas Chromatograph (GLC), equipped with Flame Photometric Detector (FPD) operated in the phosphorus mode (525 nm filter) under the following conditions. The used column was PAS: 1701 (30.00m x 0.32 mm and 0.25  $\mu$ m film thickness. Detector temperature was 250°C, injector temperature was 245°C, and the column temperature was programmed so that reaches to 190°C and hold on 2 minutes, then rose to 240°C, at a rate of 10°C min<sup>-1</sup> and hold on 5 minutes. Nitrogen carrier gas flow rate was 4 ml min<sup>-1</sup>, hydrogen flow was 75 ml min<sup>-1</sup> and air flow was 100 ml min<sup>-1</sup>.

### 2.7. Characterization of activated carbon:

#### 2.7.1. Scanning electron microscopy and Fourier transform infrared study:

Scanning electron microscopy (SEM) (JEOL 5400, Japan) analysis was carried out on ASAC to study its surface texture at 30 KV accelerated voltage. Prior to scanning, the adsorbent was coated with a thin layer of gold using a sputter coater to

make it conductive. The surface functional groups of ASAC were determined using Fourier transform infrared spectroscopy (FT-IR-4100 JASCO, Japan). FT-IR technique is an important technique used in identifying characteristic surface functional groups on the adsorbent, which in some cases are responsible for the binding of the adsorbate molecules. The spectrum was recorded from 4000 to 400 /cm adopting the KBr pellet method of sample handling.

## Results and Discussion

### 3.1. Characterization of activated carbon:

#### 3.1.1. FTIR analysis:

The FTIR spectrum analysis is important to identify the characteristic functional groups of the biosorbent, which are responsible for adsorption of pesticide molecules. The data in Fig.1 shows a broad band ranging from 3409-3350 /cm represent O-H stretching, two bands at 2807 & 2909/cm correspond to stretching of the C-H bonds of the methyl and methylene groups present in the structure. Band around 2361.41/cm is characteristic of the C≡C stretching vibration of alkyne groups Smith (1999). Peak occurring at 1529.27/cm is characteristic of C≡C stretching vibration of aromatic ring Ren *et al.*, [29]. The peak observed at 1730.8 /cm is due to C=O stretching in the ketone, aldehydes, lactones, or carboxyl groups. The appearance of bands at 900-1300 /cm could be also due to phosphorous species resulting from phosphoric acid activation. From the FTIR analysis, it is clear that some surface functional groups are present on the ASAC that might be involved in the pesticide adsorption process.

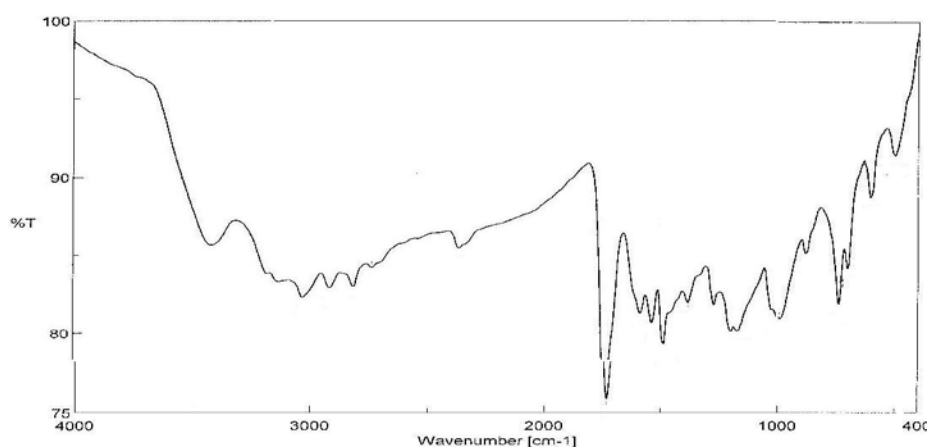


**Fig. 1:** Fourier transform infrared (FTIR) spectrum of ASAC.

#### 3.1.2. Scanning electron microscopy:

The microstructure of the ASAC was observed by SEM at 200x magnification and is shown in Fig.2.

This figure shows that the adsorbent had an irregular shape and porous surface, indicating relatively high surface areas. The size distribution of micropores of activated carbon had no definite morphology. This

observation is supported by the BET surface area of the ASAC. The values of BET surface areas and average pore diameter obtained for ASAC were  $566 \text{ m}^2/\text{g}$  and  $0.32 \text{ nm}$ , respectively. According to the IUPAC recommendation, total porosity can be

classified into three groups which were macropores ( $d > 50 \text{ nm}$ ), mesopores ( $2 < d < 50 \text{ nm}$ ) and micropores ( $d < 2 \text{ nm}$ ). Based on the average pore diameter value, ASAC falls into the category of micropores.

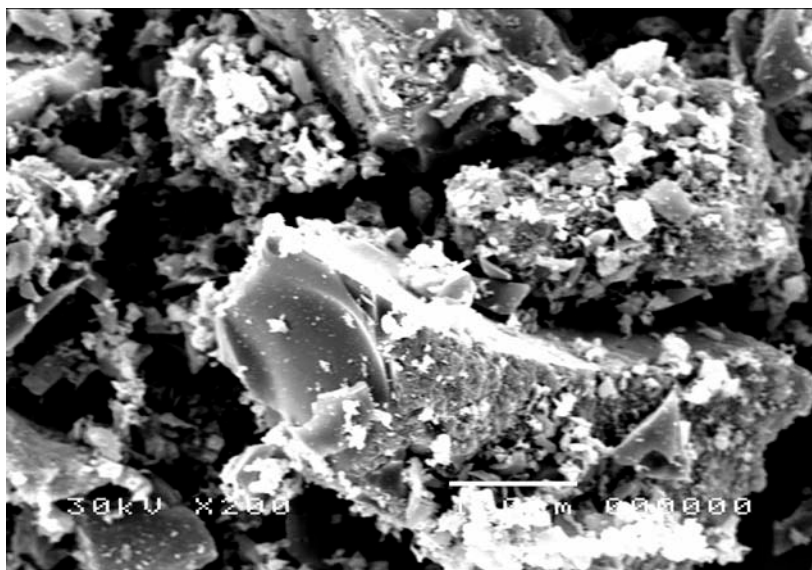


**Fig. 2:** Scanning electron microscopy (SEM) of ASAC.

### 3.2. Effect of biosorbent dose:

The effect of biosorbent dose ranging from 0.1 to 1 g/100 ml on ethoprophos biosorption is presented in Fig.3. The removal percentage of ethoprophos increased from 94.03 % to 99.90 % for biosorbent dosage of 0.1 to 1 g/100 ml, respectively.

This is due to the availability of more binding sites as the dose of biosorbent increased. However, the amount of ethoprophos adsorbed onto the sorbent,  $q$  ( $\text{mg g}^{-1}$ ), was found to decrease from 61.21 to 6.494  $\text{mg g}^{-1}$  with increasing biosorbent dose. It is due to the high number of unsaturated biosorption sites during biosorption process.

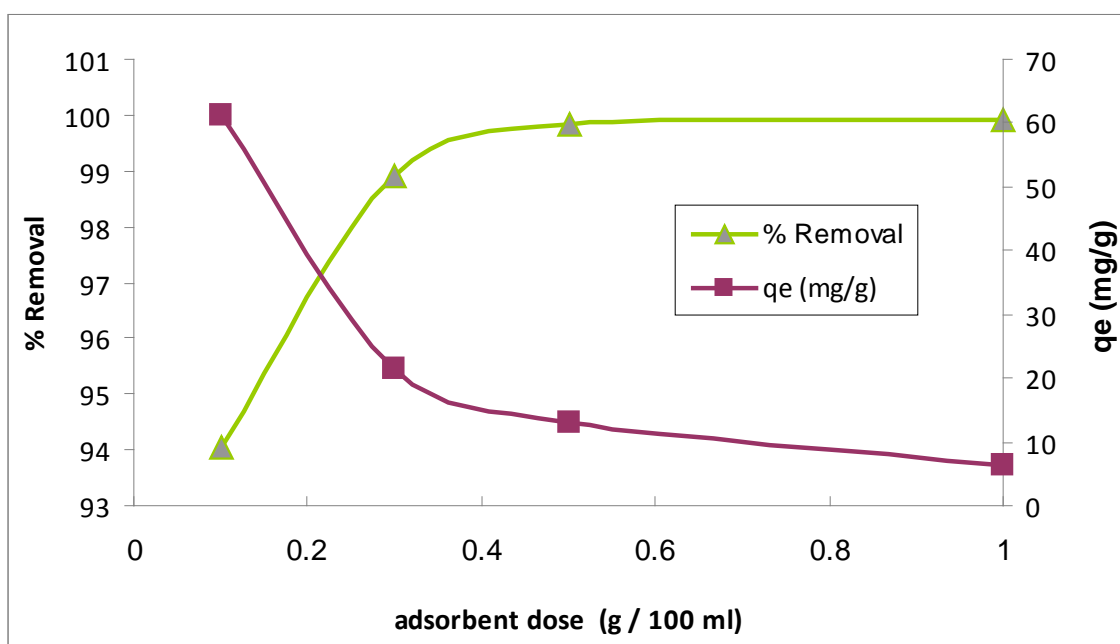


**Fig. 3:** The effect of biosorbent dose on ethoprophos removal onto ASAC ( $C_0$ : 60 mg/L, temperature:  $25 \pm 2$  °C).

### 3.3. Effect of pesticide concentration:

Biosorption of ethoprophos onto apricot stone activated carbon (ASAC) was carried out at different initial pesticide concentrations in the range of 30 to 70 mgL<sup>-1</sup>. The results are depicted in Fig 4. The adsorption capacity of ASAC increased from 5.996 to 13.978 mg g<sup>-1</sup> with increasing of the ASAC concentration. This is probably due to increase in the driving force of the concentration gradient, as an

increase in the initial pesticide concentration. However, the removal percentage of ethoprophos decreased with increasing concentration of the pesticide. At higher pesticide concentrations, lower pesticide removal percentage is probably due to the saturation of sorption sites Zeroual *et al.*, [36]. Similar results were reported by other workers for coffee bean and Polygonum orientale Baek *et al.*, [6], Wang *et al.*, [34].

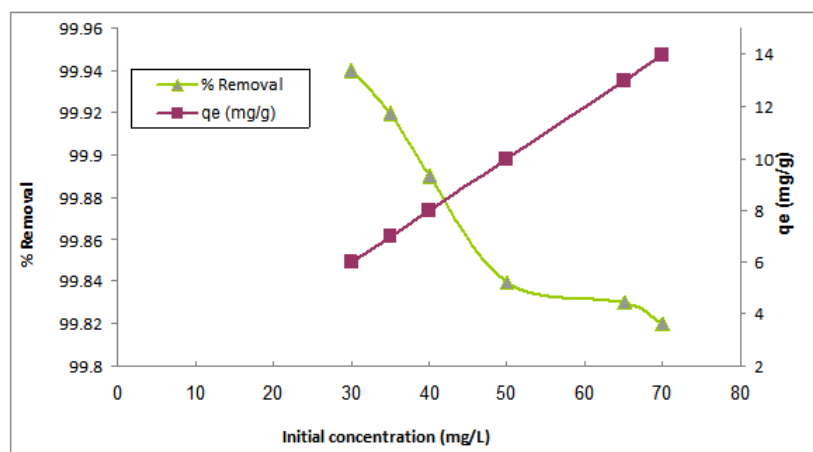


**Fig. 4:** The effect of initial concentration for removal of ethoprophos by ASAC (biosorbent dose, 0.5g/100 ml, temperature: 25 ± 2 °C).

### 3.4. Effect of contact time:

The amount of ethoprophos adsorbed onto ASAC is shown as a function of time (5-360 min). Fig 5. shows the effect of contact time on the adsorption of ethoprophos by ASAC. The pesticide adsorption rate was rapid in the initial stages of contact time and gradually decreased until equilibrium. The rapid biosorption is probably due to the abundant availability of active sites on the surface of ASAC. Afterwards with the gradual occupancy of these sites, the adsorption became less efficient. This is in accordance with the results obtained for rice husk and hazelnut shell Safa and Bhatti [30], Dogan *et al.*, [12]. It is clear from the figure that the reaction of biosorption nearly reached equilibrium within 180 min.

### 3.5. Equilibrium isotherms:

The equilibrium adsorption isotherm is of importance in the design of adsorption systems

Mahmoodi *et al.*, [24]. The equilibrium data were analyzed by the most commonly used isotherms; Langmuir and Freundlich isotherm models Langmuir [23], Freundlich [15].

The Langmuir model assumes that uptake of adsorbate occurs on a homogenous surface by monolayer adsorption without any interaction between the adsorbed ions. Also, all the binding sites of the surface have equal energy of sorption. The linear form of the Langmuir equation can be given as:

$$\frac{C_e}{q_e} = \frac{1}{Q_m b} + \frac{C_e}{Q_m} \quad (3)$$

Where  $q_e$  is the amount of pesticide adsorbed onto adsorbent at equilibrium,  $b$  is the Langmuir constant and  $q_m$  is the monolayer adsorption capacity. The plot of  $C_e/q_e$  versus  $C_e$  is employed to generate the intercept value of  $1/bq_m$  and slope of  $1/q_m$  (Fig.6).

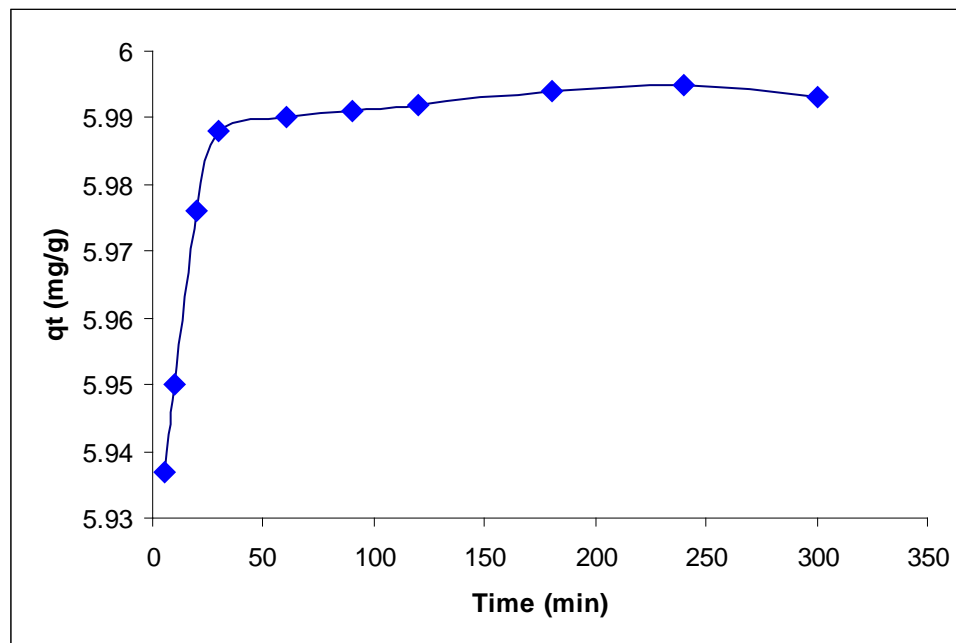


**Fig. 5:** The effect of contact time on ethoprophos removal by ASAC (biosorbent dose, 0.5g/100 ml, temperature:  $25 \pm 2$  °C).

One of the essential characteristics of this model can be expressed in terms of the dimensionless separation factor for equilibrium parameter,  $R_L$ , defined as Hall *et al.*, [17]:

$$R_L = \frac{1}{1 + bC_0} \quad (4)$$

The value of  $R_L$  indicates the type of isotherm to be irreversible ( $R_L=0$ ), favourable ( $0 < R_L < 1$ ), linear ( $R_L=1$ ) or unfavourable ( $R_L > 1$ ). The value of  $R_L$  in the present investigation was found to be 0.00039 indicating that the adsorption of ethoprophos on ASAC is favorable.

The Freundlich isotherm, on the other hand, assumes a heterogeneous sorption surface with sites that have different energies of adsorption. The Freundlich model can be represented as:

$$q_e = K_f C_e^{1/n_f} \quad (5)$$

Eq. (5) can be linearized in the logarithmic form (Eq. 6) and the Freundlich constants can be determined:

$$\log q_e = \log K_f + 1/n_f \log C_e \quad (6)$$

Where  $K_f$  is the relative adsorption capacity of adsorbent and  $1/n_f$  is a constant related to sorption intensity. The plot of  $\log q_e$  versus  $\log C_e$  should give a straight line with a slope of  $1/n_f$  and intercept of  $\log K_f$  (plot not shown). The  $1/n_f$  value was found as 0.433 in the present case. The value of  $1/n_f$  smaller than unity indicates that the adsorption process is favourable Zeroual *et al.*, [37].

### 3.6. Adsorption kinetics:

The kinetic studies provide useful data regarding the efficiency of adsorption process and feasibility of scale-up operations Calvete *et al.*, [8]. Several kinetic models are available to describe the adsorption kinetics. Mostly used models including the pseudo-first order, pseudo-second order and intraparticle diffusion were applied to the experimental data to evaluate the kinetics of ethoprophos adsorption by ASAC.

**Table 2:** Equilibrium constants for the adsorption of ethoprophos by ASAC.

| Isotherm model               | Parameters |
|------------------------------|------------|
| Langmuir isotherm            |            |
| $q_m$ (mg/g)                 | 20.04      |
| $B$ (L/mg)                   | 20.833     |
| $R^2$                        | 0.9618     |
| $R_L$                        | 0.0006     |
| Freundlich isotherm          |            |
| $K_F$ (mg/g) (mg/L) $^{1/n}$ | 33.682     |
| $1/n_f$                      | 0.4332     |
| $R^2$                        | 0.9513     |

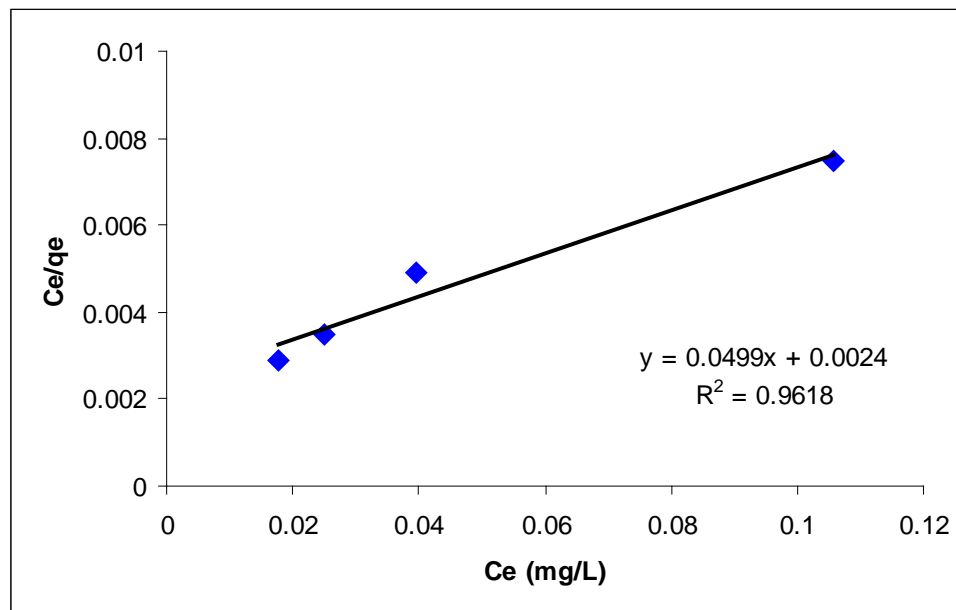


**Fig. 6:** Langmuir adsorption isotherm for ethoprophos adsorption on ASAC.

### 3.6.1. The pseudo first-order:

The pseudo-first order kinetic model can be defined as:

$$\log(q_e - q_t) = \log(q_e) - \frac{K_1}{2.303}(t) \quad (7)$$

Where  $q_e$  and  $q_t$  are the amount of ethoprophos adsorbed (mg/g) on the adsorbent at the equilibrium and at time  $t$ , respectively, and  $k_1$  is the pseudo-first order rate constant of sorption. The values of  $q_e$  and  $k_1$  can be determined from the slope and intercept of the plot obtained by plotting  $\log(q_e - q_t)$  versus  $t$  (figure not shown). The application of this equation to the data of ethoprophos on ASAC indicated the inapplicability of the model.

### 3.6.2. The pseudo-second order:

The Pseudo-second order kinetic model can be represented as:

$$\frac{t}{qt} = \frac{1}{K_2 q_e^2} + \frac{1}{q_e}(t) \quad (8)$$

Where  $K_2$  is the rate constant for the pseudo-second order kinetics (g /mg min). The linear plot of  $(t/qt)$  versus  $t$  is shown in Fig7. The initial sorption rate can be calculated using the relation Koynucu [22].

$$K_0 = K_2 q_e^2 \quad (9)$$

The parameters calculated for the pseudo-second order kinetic model are listed in Table 3. As seen from the table, due to high  $R^2$ , the pseudo-second order is predominant kinetic model for the ethoprophos adsorption by apricot stone activated carbon (ASAC).

### 3.6.3. The intraparticle diffusion model:

In order to identify the diffusion mechanism, the intraparticle diffusion model can be represented as:

$$q_t = k_i t^{1/2} + C \quad (10)$$

Where  $k_i$  is the intraparticle diffusion rate constant and  $C$  is a constant which gives information about the thickness of boundary layer. According to this model, the plot of  $q$  versus  $t^{0.5}$  yields a straight line passing through the origin if the adsorption process obeys the sole intraparticle diffusion model. However, it is not the case in Fig 8, and therefore, the intraparticle diffusion is not the only rate limiting step. It could be stated that this process is complex and may involve more than one mechanism. This is in accordance with the results obtained for *Araucaria angustifolia* and garlic peel Calvete *et al.*, [9], Hameed and Ahmad [18].

The results demonstrated that the values of coefficient of determination ( $R^2$ ) for the intraparticle diffusion was slightly lower than those of a pseudo-second order kinetic model indicating that pseudo-second order model is better obeyed than intraparticle diffusion model.

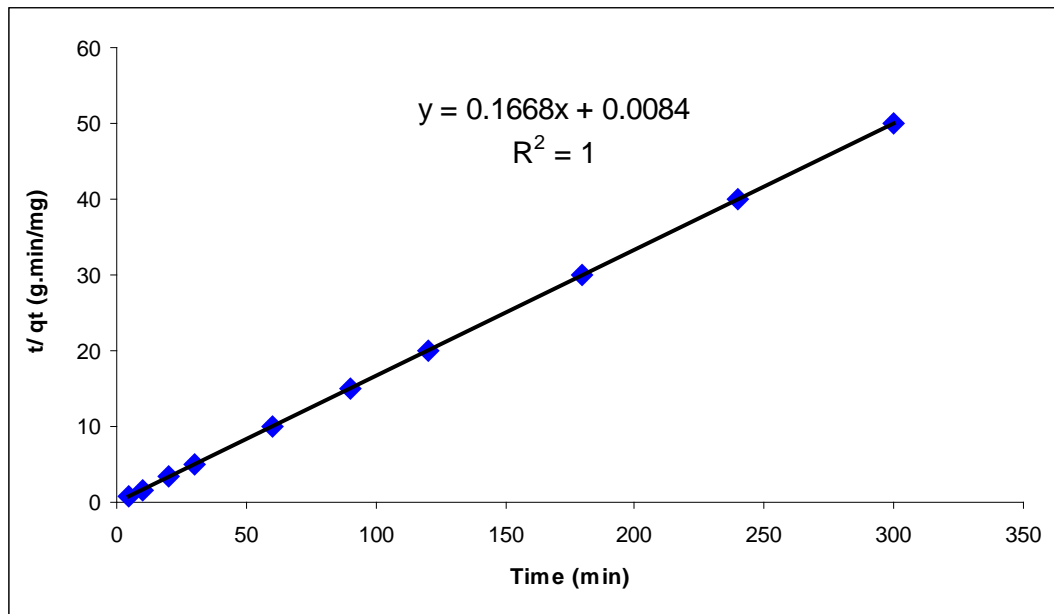


**Fig. 7:** Pseudo-second order kinetic model for adsorption of ethoprophos onto ASAC ( $C_0 = 30$  mg/L, temperature  $25 \pm ^\circ\text{C}$ ).

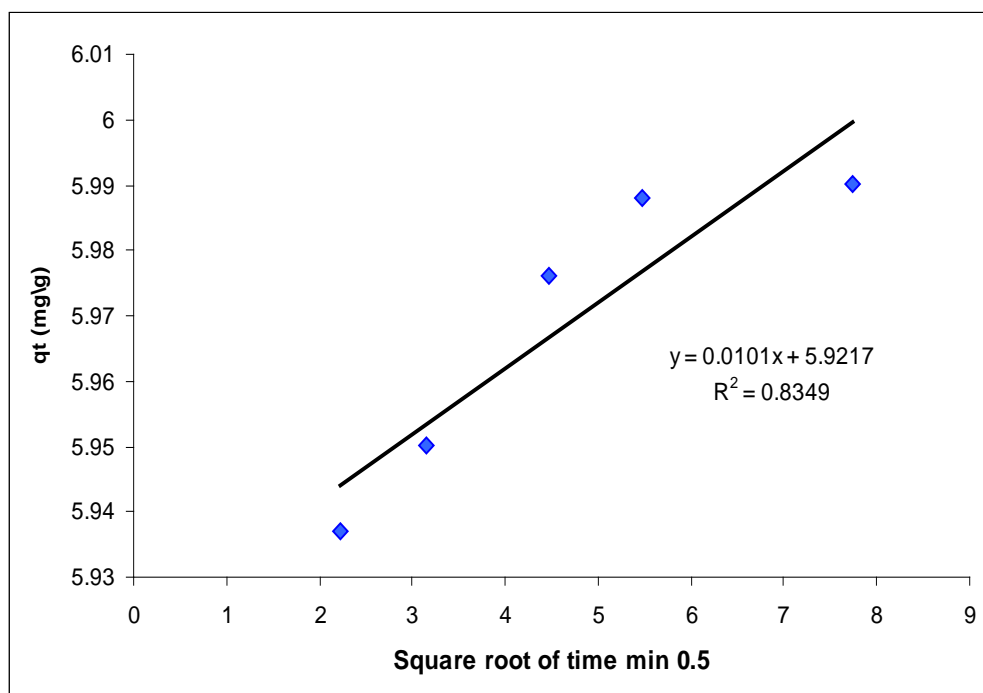


**Fig. 8:** Intraparticle diffusion for adsorption of ethoprophos onto ASAC ( $C_0 = 30$  mg/L, temperature  $25 \pm ^\circ\text{C}$ ).

**Table 3:** Kinetic parameters for the removal of ethoprophos by ASAC.

| Kinetic model                 | Parameter                        | Value  |
|-------------------------------|----------------------------------|--------|
| pseudo-second order           | $K_2$ (g/mg.min)                 | 3.32   |
|                               | $K_0$ (g/mg.min)                 | 119.12 |
|                               | $R^2$                            | 1.0000 |
|                               | $q_e$ (mg/g)                     | 5.99   |
|                               |                                  |        |
| Intraparticle diffusion model | $k_i$ (mg/g min <sup>1/2</sup> ) | 0.01   |
|                               | $R^2$                            | 0.834  |

### 3.7. Thermodynamic parameters:

The thermodynamic parameters such as free energy change ( $\Delta G^\circ$ ), enthalpy change ( $\Delta H^\circ$ ) and entropy change ( $\Delta S^\circ$ ) have a significant role to define the feasibility, spontaneity and heat change for the biosorption process and can be estimated by the following equations:

$$\Delta G^\circ = -RT \ln K_c \quad (11)$$

$$\ln K_c = \frac{\Delta S^\circ}{R} - \frac{\Delta H^\circ}{RT} \quad (12)$$

Where  $K_c$  is the Equilibrium constant ( $q_e / C_e$ ),  $\Delta G^\circ$  Gibbs free energy (Joule/mole),  $\Delta H^\circ$  Enthalpy (Joule/mole),  $\Delta S^\circ$  Entropy (Joule/ mol K), T is the

absolute temperature (K),  $C_0$  is the initial concentration of the adsorbate,  $C_{eq}$  is the equilibrium concentration, R is the gas constant.

A plot of  $\ln K_c$  versus  $1/T$  for the initial pesticide concentration of 30 mg/L was linear (Fig 9). The Values of  $\Delta H^\circ$  and  $\Delta S^\circ$  were determined from the slope and intercept of the plot and represented in Table (4).

The negative value of  $\Delta G^\circ$  at three temperatures confirms the spontaneous nature and feasibility of the biosorption process for ethoprophos pesticide onto ASAC. The positive value of  $\Delta H^\circ$  confirms that process is endothermic in nature. The positive value of entropy  $\Delta S^\circ$  shows increased randomness at the solid– solution interface during the biosorption process Kelleher *et al.*, [21].

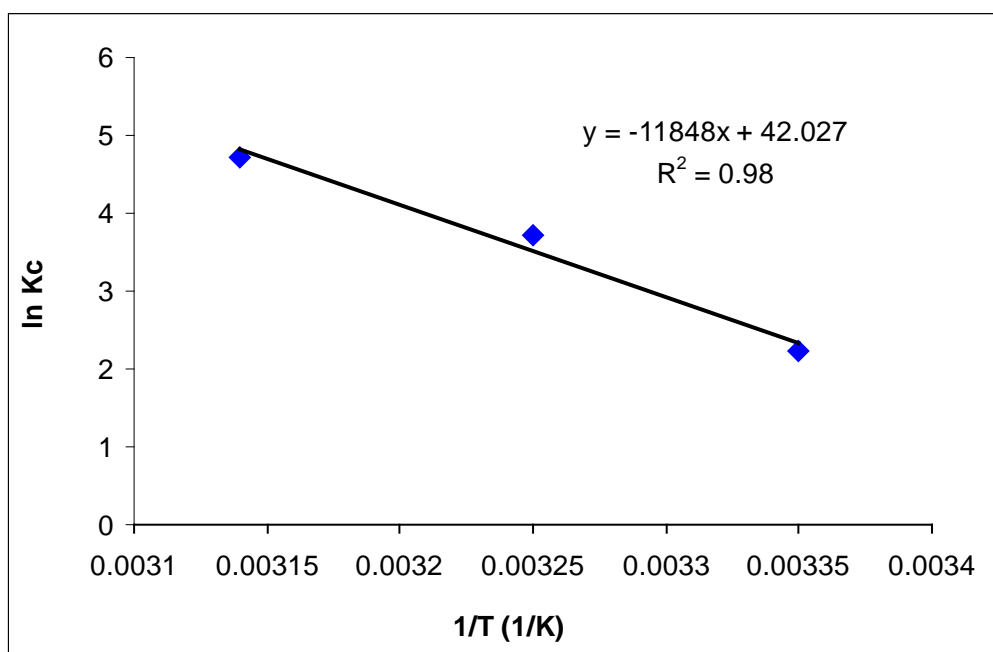


**Fig. 9:** Thermodynamic data for ethoprophos adsorption onto ASAC.

**Table 4:** Thermodynamic parameters for the adsorption of ethoprophos on ASAC.

| - $\Delta G^\circ$ (KJ/mol) |        |        | $\Delta H^\circ$ (KJ/mol) | $\Delta S^\circ$ (J/mol K) |
|-----------------------------|--------|--------|---------------------------|----------------------------|
| 298 K                       | 308 K  | 318 K  | 98.504                    | 349.412                    |
| 104.02                      | 107.52 | 111.01 |                           |                            |

### 4. Conclusions:

The present study investigated the removal of pesticide ethoprophos by the apricot stone activated carbon (ASAC) from aqueous solutions. The equilibrium data fitted well with the Langmuir isotherm. The monolayer sorption capacity of the adsorbent was found as 20.04 mg g<sup>-1</sup> by using Langmuir equation. The kinetic data were best described by the pseudo-second order model.

Thermodynamic parameters suggested that the adsorption of ethoprophos on apricot stone activated carbon was feasible, spontaneous and endothermic in

nature. The results showed that the apricot stone activated carbon as an eco-friendly and low-cost adsorbent might be a suitable alternative for the elimination of ethoprophos from aqueous solutions.

### References

1. Ahmad, M.A., R. Alrozi, 2010. Optimization of preparation conditions for mangosteen peel-based activated carbons for the removal of Remazol Brilliant Blue R using response surface methodology, Chem. Eng. J. 165: 883-890.

- Ahmad, M.A., R. Alrozi, 2011. Optimization of rambutan peel based activated carbon preparation conditions for Remazol Brilliant Blue R removal, *Chem. Eng. J.*, 166: 280-285.
- Anonymous, Agricultural Statistics, Economic Affairs Sector, Egyptian Ministry of Agriculture and land Reclamation, Cairo, 2005.
- Arslanoglu, F.N., F. Kar, N. Arslan, 2005. Adsorption of dark coloured compounds from peach pulp by using powdered activated carbon, *J. Food Eng.*, 71: 156-163.
- Baccar, R., P. Blanquez, J. Bouzid, M. Feki, M. Sarra, 2010. Equilibrium, thermodynamic and kinetic studies on adsorption of commercial dye by activated carbon derived from olive-waste cakes, *Chem. Eng. J.*, 165: 457-464.
- Baek, M.H., C.O. Ijagbemi, O. Se-Jin, D.S. Kim, 2010. Removal of Malachite Green from aqueous solution using degreased coffee bean, *J. Hazard. Mater.*, 176: 820-828.
- Banasiak, L.J., B. Van der Bruggen, A.I. Schäfer, 2011. Sorption of pesticide endosulfan by electro dialysis membranes, *Chem. Eng. J.*, 166: 233-239.
- Calvete, T., E.C. Lima, N.F. Cardoso, J.C.P. Vaghetti, S.L.P. Dias, F.A. Pavan, 2010. Application of carbon adsorbents prepared from Brazilian-pine fruit shell for the removal of reactive orange 16 from aqueous solution: kinetic, equilibrium, and thermodynamic studies, *J. Environ. Manage.*, 91: 1695-1706.
- Calvete, T., E.C. Lima, N.F. Cardoso, S.L.P. Dias, F.A. Pavan, 2009. Application of carbon adsorbents prepared from the Brazilian-pine fruit shell for removal of Procion Red MX 3B from aqueous solution-kinetic, equilibrium and thermodynamic studies, *Chem. Eng. J.*, 155: 627-636.
- CDS.Tomlin, 2004. The e-Pesticides Manual, version 3.0, 13th ed., BCPC (British Crop Protection Council), Copyright ©.
- Derylo-Marczewska, A., M. Blachnio, A.W. Marczewski, A. Swiatkowski, B. Tarasiuk, 2010. Adsorption of selected herbicides from aqueous solutions on activated carbon, *J. Therm. Anal. Calorim.*, 101: 785-794.
- Dogan, M., H. Abak, M. Alkan, 2009. Adsorption of methylene blue onto hazelnut shell: kinetics, mechanism and activation parameters, *J. Hazard. Mater.*, 164: 172-181.
- Dolas, H., O. Sahin, C. Saka, H. Demir, 2011. A new method on producing high surface area activated carbon: the effect of salt on the surface area and the pore size distribution of activated carbon prepared from pistachio shell, *Chem. Eng. J.*, 166: 191-197.
- Farooq, U., J.A. Kozinski, M.A. Khan, M. Athar, 2010. *Bioresour. Technol.*, 101: 5043-5053.
- Freundlich, H., 1906. Over the adsorption in the solution, *J. Phys. Chem.*, 57: 385-470.
- Gong, J., C. Yang, W. Pu, J. Zhang, 2011. Liquid phase deposition of tungsten doped TiO<sub>2</sub> films for visible light photoelectrocatalytic degradation of dodecyl- benzenesulfonate, *Chem. Eng. J.*, 167: 190-197.
- Hall, K.R., L.C. Eagleton, A. Acrivos, T. Vermeulen, 1966. Pore and solid-diffusion kinetics in fixed-bed adsorption under constant-pattern conditions, *I&EC Fundam.*, 5: 212-223.
- Hameed, B.H. and A.A. Ahmad, 2009. Batch adsorption of methylene blue from aqueous solution by garlic peel, an agricultural waste biomass, *J. Hazard. Mater.*, 164: 870-875.
- International Agency for Research on Cancer (IARC), Overall evaluations of carcinogenicity: An updating of IARC monographs volumes 1 to 42, Supplement 7, WHO, Lyon, France., 1987. <http://monographs.arc.fr/ENG/Monographs/PDFs/index.php>.
- Katsumata, H., T. Kobayashi, S. Kaneco, T. Suzuki, K. Ohta, 2011. Degradation of linuron by ultrasound combined with photo-Fenton treatment, *Chem. Eng. J.*, 166: 468-473.
- Kelleher, B.P., M.N. O'Callaghan, M.J. Leahy, T.F. O'Dwyer, J.J. Leahy, 2002. The use of fly ash from the combustion of poultry litter for the adsorption of chromium(III) from aqueous solution. *J Chem Technol Biotechnol.*, 77: 1212-1218.
- Koynucu, H., 2008. Adsorption Kinetics of 3-hydroxybenzaldehyde on native and activated bentonite, *Appl. Clay Sci.*, 38: 279.
- Langmuir, I., 1918. The adsorption of gases on plane surfaces of glass, mica and platinum, *J. Am. Chem. Soc.*, 40: 1361-1403.
- Mahmoodi, N.M., R. Salehi, M. Arami, 2011. Binary system dye removal from colored textile wastewater using activated carbon: kinetic and isotherm studies, *Desalination*, 272: 187-195.
- Maldonado, M.I., S. Malato, L.A. Perez-Estrada, I. Gernjak, X. Oller, J. Domenech, 2006. Peral, Partial degradation of five pesticides and an industrial pollutant by ozonation in a pilot-plant scale reactor, *J. Hazard Mater.*, 38: 363-369.
- Njoku, V.O. and B.H. Hameed, 2011. Preparation and characterization of activated carbon from corncob by chemical activation with H<sub>3</sub>PO<sub>4</sub> for 2,4-dichlorophenoxyacetic acid adsorption, *Chem. Eng. J.*, 173: 391-399.
- Philip, H.H., E.M. Michalenko, W.F. Jarvis, D.K. Basu, G.W. Sage, W.M. Meyland, J.A. Beauman, D.A. Gray (Eds.), 1991. *Handbook of Environmental Fate and Exposure Data for Organic Chemicals*, vol. III, Lewis, Chelsea, MI.

28. Rajashekara, H.M., H.K. Murthy, Manonmani, 2007. Aerobic degradation of technical hexachlorocyclohexane by a defined microbial consortium, *J. Hazard Mater*, 149: 18-25.
29. Ren, L., J. Zhang, Y. Li, C. Zhang, 2011. Preparation and evaluation of cattailfiber -based activated carbon for 2,4-dichlorophenol and 2,4,6-trichlorophenol removal, *Chem. Eng. J.*, 168: 553-561.
30. Safa, Y. and H.N. Bhatti, 2011. Kinetic and thermodynamic modeling for the removal of Direct Red-31 and Direct Orange-26 dyes from aqueous solutions by rice husk, *Desalination*, 272: 313-322.
31. Smith, B., 1999. *Infrared Spectral Interpretation: A Systematic Approach*, CRC Press, Boca Raton.
32. Sun, Y. and P.A. Webley, 2010. Preparation of activated carbons from corncob with large specific surface area by a variety of chemical activators and their application in gas storage, *Chem. Eng. J.*, 162: 883-892.
33. Uğurlu, M., M.H. Karaoğlu, 2011. TiO<sub>2</sub> supported on sepiolite: preparation, structural and thermal characterization and catalytic behaviour in photocatalytic treatment of phenol and lignin from olive mill wastewater, *Chem. Eng. J.*, 166: 859-867.
34. Wang, L., J. Zhang, R. Zhao, C. Li, Y. Li, C. Zhang, 2010. Adsorption of basic dyes on activated carbon prepared from *Polygonum orientale* Linn: equilibrium, kinetic and thermodynamic studies, *Desalination*, 254: 68-74.
35. Yang, J. and K. Qiu, 2010. Preparation of activated carbons from walnut shells via vacuum chemical activation and their application for methylene blue removal, *Chem. Eng. J.*, 165: 209-217.
36. Zeroual, Y., B.S. Kim, C.S. Kim, M. Blaghen, K.M. Lee, 2006. Biosorption of bromophenol blue from aqueous solutions by *Rhizopus stolonifer* biomass, *Water Air Soil Pollut.*, 177: 135-146.
37. Zeroual, Y., B.S. Kim, C.S. Kim, M. Blaghen, K.M. Lee, 2006. Biosorption of bromophenol blue from aqueous solutions by *Rhizopus stolonifer* biomass, *Water Air Soil Pollut.*, 177: 135-146.
38. Zhou, T., T.T. Lim, S.S. Chin, A.G. Fane, 2011. Treatment of organics in reverse osmosis concentrate from a municipal wastewater reclamation plant: feasibility test of advanced oxidation processes with/without pretreatment, *Chem. Eng. J.*, 166: 932-939.